Early Detection of Chemoradioresponse in Esophageal Carcinoma by 3′-Deoxy-3′-^{3}H-Fluorothymidine Using Preclinical Tumor Models

Smith Apisarnthanarax,[1] Mian M. Alauddin,[2] Firas Mourtada,[3] Hisanori Ariga,[1] Uma Raju,[1] Osama Mawlawi,[4] Dongmei Han,[2] William G. Bornmann,[2] Jaffer A. Ajani,[5] Luka Milas,[1] Juri G. Gelovani,[2] and K.S. Clifford Chao[1]

Abstract

Purpose: Early identification of esophageal cancer patients who are responding or resistant to combined chemoradiotherapy may lead to individualized therapeutic approaches and improved clinical outcomes. We assessed the ability of 3′-deoxy-3′-^{18}F-fluorothymidine positron emission tomography (FLT-PET) to detect early changes in tumor proliferation after chemoradiotherapy in experimental models of esophageal carcinoma.

Experimental Design: The *in vitro* and *ex vivo* tumor uptake of [^{3}H]FLT in SEG-1 human esophageal adenocarcinoma cells were studied at various early time points after docetaxel plus irradiation and validated with conventional assessments of cellular proliferation [thymidine (Thd) and Ki-67] and [^{18}F]FLT micro-PET imaging. Imaging-histologic correlation was determined by comparing spatial Ki-67 and [^{18}F]FLT distribution in autoradiographs. Comparison with fluorodeoxyglucose (FDG) was done in all experiments.

Results: *In vitro* [^{3}H]FLT and [^{3}H]Thd uptake rapidly decreased in SEG-1 cells 24 hours after docetaxel with a maximal reduction of over 5-fold ($P = 0.005$). The [^{3}H]FLT tumor-to-muscle uptake ratio in xenografts declined by 75% compared with baseline ($P < 0.005$) by 2 days after chemoradiotherapy, despite the lack of change in tumor size. In contrast, the decline of [^{3}H]FDG uptake was gradual and less pronounced. Tumor uptake of [^{3}H]FLT was more closely correlated with Ki-67 expression ($r = 0.89$, $P < 0.001$) than was [^{3}H]FDG ($r = 0.39$, $P = 0.08$). Micro-PET images depicted similar trends in reduction of [^{18}F]FLT and [^{18}F]FDG tumor uptake. Autoradiographs displayed spatial correlations between [^{18}F]FLT uptake and histologic Ki-67 distribution in preliminary studies.

Conclusions: FLT-PET is suitable and more specific than FDG-PET for depicting early reductions in tumor proliferation that precede tumor size changes after chemoradiotherapy.

Esophageal cancer is one of the most lethal human malignancies. Achievement of pathologic complete response after neoadjuvant chemoradiotherapy in esophageal cancer patients has been shown to be associated with improved clinical outcomes (1–4). Methods to reliably evaluate and predict the proportion of residual cancer in the esophagus after chemoradiotherapy, however, are currently lacking. The ability to predict which patients will respond to chemoradiotherapy or develop resistance to it before surgery would be invaluable for individualizing therapeutic approaches and avoiding overtreatment and undertreatment. Therefore, the need for a noninvasive tool that accurately predicts response early during the course of preoperative therapy is widely acknowledged.

Conventional anatomic imaging modalities, such as computed tomography and endoscopic ultrasonography, depict cancer response as changes in tumor size and composition, which may occur only after weeks or months following therapy, and are not ideally suitable for early prediction of response in esophageal cancer. Computed tomography is inaccurate and endoscopic ultrasonography is not always feasible in this setting (5). Positron emission tomography (PET), with the glucose analogue [^{18}F]fluorodeoxyglucose (FDG), addresses these inherent limitations in anatomic imaging, but may be limited in distinguishing proliferating tumor cells from inflammatory tissue (6–8). Other radiolabeled molecular markers may improve the specificity and accuracy of early assessment of treatment response.

Because deregulated proliferation is one of the hallmarks of cancer and a high tumor proliferative rate is associated with

Authors' Affiliations: Departments of [1]Radiation Oncology, [2]Experimental Diagnostic Imaging, [3]Radiation Physics, [4]Imaging Physics, and [5]GI Medical Oncology, The University of Texas M.D. Anderson Cancer Center, Houston, Texas

Received 12/16/05; revised 4/17/06; accepted 5/22/06.

Grant support: NIH/National Cancer Institute grants CA89198 and P50 CA97007.

The costs of publication of this article were defrayed in part by the payment of page charges. This article must therefore be hereby marked *advertisement* in accordance with 18 U.S.C. Section 1734 solely to indicate this fact.

Requests for reprints: K.S. Clifford Chao, Department of Radiation Oncology, The University of Texas M.D. Anderson Cancer Center, 1515 Holcombe Boulevard, Houston, TX 77030. Phone: 713-563-2300; Fax: 713-563-2368; E-mail: cchao@mdanderson.org.

doi:10.1158/1078-0432.CCR-05-2720

aggressive biological behavior and poor response to therapy (9, 10), imaging the proliferative state of cancer cells is of great interest. Recently, 3′-deoxy-3′-^{18}F-fluorothymidine ([^{18}F]FLT), a pyrimidine nucleoside analogue, has been validated in several *in vitro* and *in vivo* studies as a promising PET radiopharmaceutical for imaging proliferation and monitoring tumor response (11–19). The basis of FLT-PET as a surrogate measure of cancer cell proliferation is dependent on the monophosphorylation of FLT by the thymidine kinase 1 (TK1) enzyme, which results in intracellular trapping of FLT (20). TK1 is virtually absent in quiescent cells but differentially expressed in the late G_1 and S phases of the cell cycle (21, 22).

Although FLT-PET has been used to assess proliferation and response to therapy (11, 12, 15–19), no study to date has examined FLT-PET for monitoring response to chemotherapy in combination with radiation. We hypothesize that FLT-PET depicts early changes in the proliferative state of esophageal cancer after chemoradiotherapy. To test this hypothesis, we developed experimental *in vitro* and murine models of esophageal cancer and used a treatment regimen consisting of docetaxel, a semisynthetic taxane (23), and irradiation. Docetaxel in combination with irradiation has been investigated in preclinical studies (23–28) and used in the clinic to produce an ~25% pathologic complete response rate in esophageal cancer (29–31). The main objective of this study is to determine whether FLT-PET is suitable and more specific than FDG-PET as a surrogate marker of chemoradioresponse for depicting early reductions in tumor proliferation that precede tumor size changes.

Materials and Methods

Radiopharmaceuticals. Methyl-^{3}H-thymidine ([^{3}H]Thd; specific activity, 65 Ci/mmol), methyl-^{3}H(*N*)-3′-fluoro-3′-deoxythymidine ([^{3}H]FLT; specific activity, 3.4 Ci/mmol), and 5,6-^{3}H-2-fluoro-2-DDG ([^{3}H]FDG; specific activity, 60 Ci/mmol) were purchased from Sigma-Aldrich (Milwaukee, WI), Moravek Biochemicals (Brea, CA), and American Radiolabeled Chemicals, Inc. (St. Louis, MO), respectively. [^{18}F]FDG was purchased from PET NET-CTI (Knoxville, TN); specific activity was estimated to be >2 Ci/μmol. [^{18}F]FLT was synthesized by radiofluorination of the 3-*N*-Boc-1[5-*O*-(44′-dimethoxytrityl)-3-*O*-nosyl-2-deoxy-β-D-lyxofuranosyl]-thymine precursor as previously described (32). Analytic HPLC showed the product to be >99% radiochemically pure. Radiochemical yield was 7%, and specific activity was estimated to be >2 Ci/μmol.

Cells and cell culture. SEG-1 cells, derived from a human Barrett's-associated adenocarcinoma of the distal esophagus (33), were maintained and grown in DMEM/F12 culture medium supplemented with 10% fetal bovine serum, 1% penicillin/streptomycin, and 1% glutamine. Cultures were kept in a humidified 5% CO_2 incubator at 37°C. For cell cycle analysis and radiotracer uptake experiments, 1×10^6 cells were seeded onto 60-mm culture dishes, and 5×10^5 cells were seeded onto six-well plates, respectively.

In vitro ***treatment with chemoradiation.*** A single dose of 10 nmol/L docetaxel (Fluka, Sigma Chemical Co., St. Louis, MO) was added to the culture medium. Twenty-four hours after docetaxel treatment, the cells were irradiated with a single dose of 8 Gy using a ^{137}Cs source (3.7 Gy/min). All control wells were treated with PBS. The concentration of docetaxel and dose of radiation were chosen based on previously published work by Dunne et al. (24) and preliminary data demonstrating cytostatic doses of docetaxel and radiation (data not shown).

In vitro ***uptake of radiotracers.*** Cellular uptake of radiotracers was determined according to methods previously described (34) with some modifications. At 0, 4, 12, and 24 hours after docetaxel treatment and 4, 12, 24, and 48 hours after irradiation, 0.2 μCi [^{3}H]Thd, [^{3}H]FLT, or [^{3}H]FDG was added to the medium of each well and incubated for 60 minutes. Untreated wells served as controls, which were incubated with the radiotracers as described for the treated cells. After incubation, the medium was rapidly removed and rinsed with cold PBS. The cells were harvested by gentle scraping, centrifuged, and weighed and assayed for radioactivity after removal of excess supernatant. The cell pellets and the media samples were solubilized with Soluene 350 and mixed with a liquid scintillation cocktail (Ultima Gold, Packard, Meridian, CT). Radioactivity was measured using a liquid scintillation counter (Tri-Carb 2100TR, Packard) and expressed as dpm. Radiotracer uptake was expressed as cell-to-media ratio: (dpm/g cell) / (dpm/mL medium). Experiments were done and repeated in triplicate.

Cell cycle analysis. At various time points (0, 4, and 24 hours after docetaxel treatment and 24 hours after irradiation), cells were harvested by trypsinization, resuspended in growth medium, resuspended in 2 mL PBS, and fixed by the addition of ice-cold 95% ethanol to 60% while being vortexed. Cells were stored in ethanol overnight at −20°C before staining, then washed and resuspended in PBS containing 10 μg/mL propidium iodide and 250 μg/mL RNase A. Cells were incubated at 37°C for 15 minutes before flow cytometric analysis using a Coulter EPICS Profile instrument (Beckman Coulter, Inc., Fullerton, CA). Cell cycle distributions were determined from histograms using Multicycle (Phoenix Flow Systems, San Diego, CA).

Animal tumor model. Male Swiss *nu/nu* mice from our own specific pathogen-free mouse colony were used at an age of 5 months. Mice were housed three to five per cage; fed sterilized, pelleted food (Agway, Inc., Syracuse, NY), and sterile water *ad libitum*; and exposed to a 12-hour light/dark cycle. The experimental protocol was approved by the Institutional Animal Care and Use Committee. Mice were maintained in a fully accredited animal facility (American Association for Accreditation of Laboratory Animal Care) and in accordance with present regulations and standards of the U.S. Department of Health and Human Services. Solitary SEG-1 tumor xenografts were generated in the right hind limbs of the mice by 10 μL i.m. injection of a single-cell suspension of 1×10^6 tumor cells. After tumors had grown to a mean diameter of 8 mm as measured in three orthogonal diameters with Vernier calipers, mice were randomized to treatment versus control groups. Mice were treated with either docetaxel alone, radiation alone, docetaxel followed by radiation, or PBS ($n = 8$).

Chemoradiation treatment of xenografts. Mice were treated with docetaxel and radiation as described previously (26). Tumors were locally irradiated 24 hours after docetaxel treatment (33 mg/kg i.v. via tail vein) with a single dose of 15 Gy using a small animal ^{137}Cs irradiator. Irradiations were given under ambient air breathing conditions at a dose rate of 5.4 Gy/min. During irradiation, the mice were mechanically immobilized (unanesthetized) on a jig, and the tumor was centered in a 3-cm-diameter circular field. Tumor response to treatment was assessed by tumor growth delay as previously described (26).

Immunohistochemical staining for proliferation. Excised tumors were fixed in 10% neutral buffered formalin and embedded in paraffin blocks, from which 4-μm sections were cut for H&E and immunohistochemical staining. A section from each specimen was labeled using the monoclonal antibody B56 (BD PharMingen, San Diego, CA), which recognizes the nuclear proliferation associated Ki-67 antigen (35), and visualized using the Vectastain ABC kit with 3,3′-diaminobenzidine (Vector Laboratories, CA) and hematoxylin counterstain. Ki-67 expression was quantified according to previously described methods with modifications (36). The fraction of Ki-67-labeled tumor cells was assessed by microscopic examination of stained sections at ×400 magnification. Five fields of nonnecrotic areas were randomly selected in each specimen, and in each field, the numbers of Ki-67-labeled cells were recorded as numbers per 200 to 300 nuclei scored and expressed as labeling index percentages (LI_{Ki-67}).

Radiotracer uptake in tumor tissue. In SEG-1-bearing mice, tumor uptake of [^{3}H]FLT or [^{3}H]FDG was assessed at 1, 2, and 4 days after chemoradiotherapy (n = 5). A bolus injection of [^{3}H]FLT or [^{3}H]FDG was administered to the mice i.v. via the lateral tail vein at a dose of 1 μCi in 200 μL. The mice were sacrificed 60 minutes after radiotracer injection by cervical dislocation. Muscle and tumor tissue were rapidly harvested, weighed, and solubilized with Solvable (Perkin-Elmer, Boston, MA). Radioactivity in the samples was measured using a Tri-Carb 2100TR liquid scintillation counter (Packard), and the results were expressed as percentage injected dose per gram of tissue (%ID/g). Uptake of [^{3}H]FLT was compared with LI_{Ki-67} within the same tumors.

Micro-PET imaging and analysis. Untreated and chemoradiotherapy-treated mice were imaged on a micro-PET R4 scanner (Concorde Microsystems, Knoxville, TN). The animals (n = 2) were first anesthetized and injected with 7 MBq (200 μCi) of either [^{18}F]FLT or [^{18}F]FDG. Sixty minutes after injection, the animals were positioned in the field of view of the scanner and imaged for 15 minutes. Care was taken to reproduce the animal positioning between the [^{18}F]FLT and [^{18}F]FDG imaging sessions. The acquired list data was then histogrammed into a single frame using Fourier rebinning, and the images were reconstructed into a 128 × 128 × 63 (0.72 × 0.72 × 1.3 mm) matrix using ordered subset expectation maximization. All corrections for attenuation, scatter, dead time, and randoms were applied to generate quantifiable images. Regions of interest were then drawn over the tumor and muscle tissue without including their respective visible boundaries and an average value within the regions of interest was generated. A ratio of tumor-to-muscle (T/M) was calculated to eliminate the dependency on the injected activity. This ratio was evaluated before and after treatment as an indicator of treatment response.

Imaging-histologic correlation with autoradiography. Autoradiography was done only on tumors from mice injected with [^{18}F]FLT. Upon completion of the micro-PET imaging studies, tumors were removed from mice and immediately frozen and processed. Sliced 8-μm sections were fixed in cold acetone, dried, and exposed to a multipurpose storage phosphor screen (Amersham Biosciences, Piscataway, NJ) overnight. A Typhoon 9400 storage phosphor screen imager (Amersham Biosciences) was used to generate digital autoradiographs and detect the distribution of radionuclide activity localized in each section. After complete radioactive decay of [^{18}F]FLT, these same sections were processed for Ki-67 immunohistochemical staining as previously described (31, 32). Spatial correlations between regions of high, intermediate, and low intensity [^{18}F]FLT uptake and Ki-67 expression were examined.

Statistical analysis. Statistical comparisons between controls and treated groups were calculated using the two-sided Student's t test for changes in tumor size and LI_{Ki-67}. Single-factor ANOVA was used to compare *in vitro* and *in vivo* radiotracer uptake before and after treatment. Correlations between histologic and radiotracer uptake findings were tested using linear regression analysis. All quantitative data were reported as mean ± SE unless otherwise specified. $P < 0.05$ was considered to be statistically significant.

Results

Cellular uptake of radiotracers* in vitro *after chemoradiotherapy. Figure 1 shows the cellular uptake of [^{3}H]Thd, [^{3}H]FLT, and [^{3}H]FDG in SEG-1 cells after treatment with docetaxel and radiation. The data were compared with untreated cell uptake in percentage. Although baseline cellular uptake of [^{3}H]FLT was 5.6-fold lower than that of [^{3}H]Thd (3.92 ± 0.18 versus 21.80 ± 0.22 cell/medium dpm, respectively), the dynamics of [^{3}H]FLT uptake after treatment (Fig. 1B) closely resembled that of [^{3}H]Thd uptake (Fig. 1A). Similar to [^{3}H]Thd, docetaxel initially increased [^{3}H]FLT uptake from a baseline of 3.92 ± 0.18 to a peak of 6.34 ± 0.08 at 12 hours (+62%, P = 0.008).

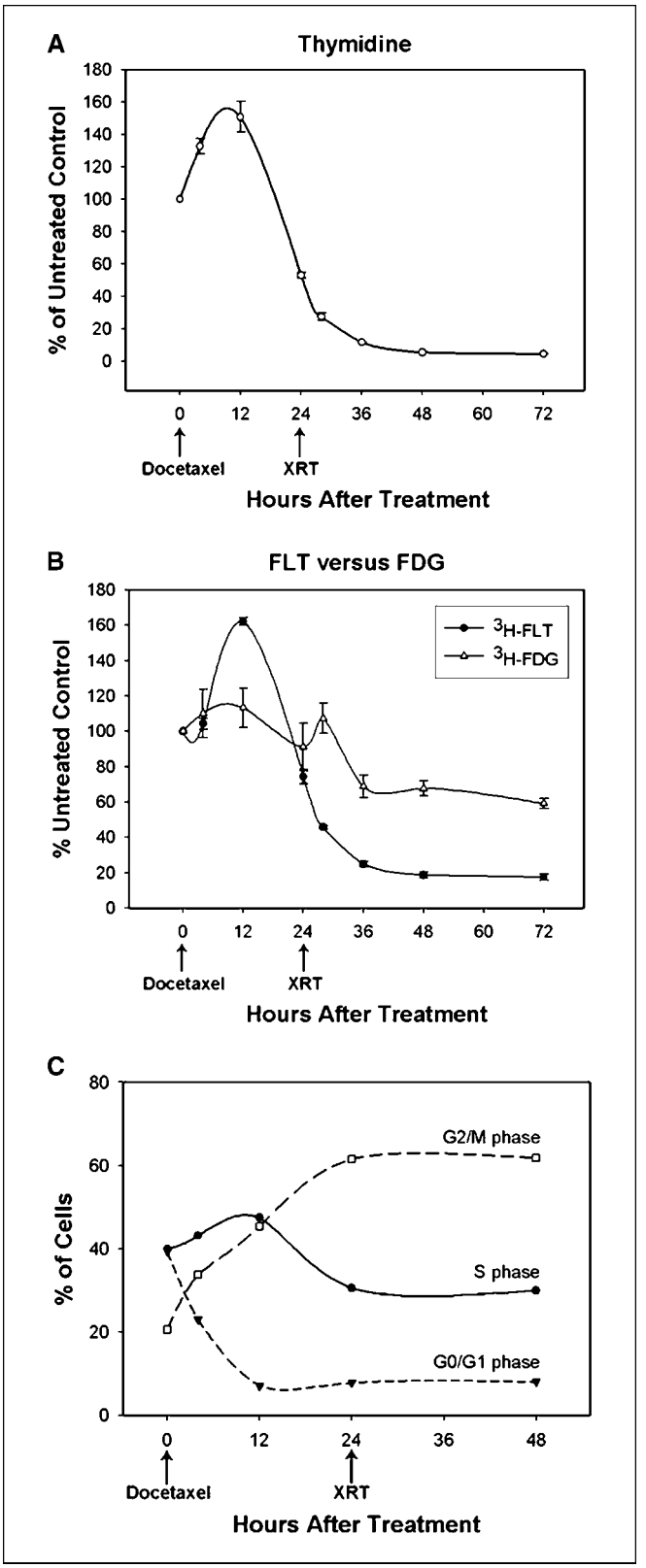

Fig. 1. Cellular uptake of [^{3}H]Thd, [^{3}H]FLT, and [^{3}H]FDG in SEG-1 cells and cell cycle analysis after docetaxel and radiation *in vitro*. Plated SEG-1 cells were treated with 10 nmol/L docetaxel (0 hour) followed by 15 Gy irradiation (*XRT*; 24 hours). *A,* [^{3}H]Thd cellular uptake served as the gold standard measure of proliferative activity. *B,* [^{3}H]FLT and [^{3}H]FDG cellular uptake. *C,* flow cytometric analysis of cell cycle distributions. Experiments were done in triplicates and repeated. Points, mean; bars, SE. *P* values were derived by ANOVA.

The uptake subsequently declined rapidly to 2.92 ± 0.16 (−26%, P = 0.005) at 24 hours and continued to steadily decrease to 0.68 ± 0.06 at 72 hours after docetaxel treatment (24 hours after irradiation) compared with baseline uptake (−83%, P = 0.006).

The cellular uptake dynamics of [^{3}H]FDG after treatment was characterized by a delayed and less pronounced decrease compared with [^{3}H]Thd and [^{3}H]FLT (Fig. 1B). A statistically significant reduction in [^{3}H]FDG uptake was not observed until 36 hours after docetaxel (12 hours after irradiation). [^{3}H]FDG uptake declined by 31% compared with baseline (P = 0.01) at 36 hours and continued to gradually decrease an additional 10% compared with baseline (P = 0.004) at 72 hours after docetaxel (48 hours after irradiation).

Cell cycle analysis. To examine the effects of docetaxel and irradiation on cell cycle distribution, flow cytometric analysis was done on SEG-1 cells *in vitro* after treatment (Fig. 1C). The percentage of cells in G_2-M phase was elevated from a baseline of 20.61% to 61.88% at 48 hours after docetaxel treatment (24 hours after irradiation), whereas cells in G_0-G_1 phase were markedly reduced to 8.09% from a baseline of 39.43%. The effect of docetaxel and radiation on S-phase cells was similar to the alterations in [^{3}H]Thd and [^{3}H]FLT cellular uptake. The percentage of cells in S phase initially increased to 47.46% at 12 hours after docetaxel from a baseline of 39.96% and subsequently declined to 30.03% at 48 hours after docetaxel treatment (24 hours after irradiation).

Effect of chemoradiotherapy on xenograft tumor size and proliferation. The antitumor effect of docetaxel and radiation on SEG-1 tumor-bearing mice, assessed by tumor growth delay, is shown in Fig. 2A. Although the untreated group tumors continued to increase in size during the first few days after treatment, the tumors in the docetaxel plus irradiation group maintained stable sizes: 0 days (pretreatment), 7.98 ± 0.05 mm; 2 days, 8.12 ± 0.08 mm; and 4 days, 7.96 ± 0.12 mm. A significant reduction in tumor size was observed at 8 days with a maximal decline at 10 days in this treatment group (P = 0.03).

Because there was no significant change in tumor size in the first 4 days after chemoradiotherapy, we stained and quantified histologic sections of SEG-1 tumors for Ki-67 to assess temporal changes in tumor proliferation after treatment during this time period (Fig. 2B-C). The baseline $LI_{Ki\text{-}67}$ of pretreatment SEG-1 tumors was high at 92.10 ± 1.49%. A statistically significant decrease in tumor proliferation by 11% (P = 0.02) was observed as early as 4 hours after treatment compared with pretreatment $LI_{Ki\text{-}67}$ (data not shown). $LI_{Ki\text{-}67}$ in treated tumors continued to decline rapidly by 87% to 12.43 ± 1.05% at 96 hours compared with untreated tumors (P < 0.001).

Ex vivo *uptake of [^{3}H]FLT and [^{3}H]FDG in tumors after chemoradiotherapy and correlation with proliferative markers.* Treatment with docetaxel plus radiation resulted in decreases for both [^{3}H]FLT and [^{3}H]FDG tumor uptake (Fig. 3). Absolute tumor uptake of [^{3}H]FLT after treatment was characterized by a statistically significant steep decline compared with pretreatment tumors at 1 day (−72%, P = 0.006), followed by a continued stable decline (2 days, −75%; 4 days, −76%; P < 0.005). The decrease in [^{3}H]FDG tumor uptake after treatment, however, was less pronounced, reaching a statistically insignificant decrease by 15% at 4 days compared with pretreatment tumors. Figure 3A summarizes changes in [^{3}H]FLT and [^{3}H]FDG tumor uptake; in addition, tumor size and Ki-67 expression changes are charted for correlation of radiotracer uptake with independent measures of tumor response. The [^{3}H]FLT T/M uptake ratio decreased by 57% at 1 day, 80% at 2 days, and 88% at 4 days in treated tumors compared with that of pretreatment tumors (ANOVA, P < 0.001; Fig. 3B). In contrast, the [^{3}H]FDG T/M uptake ratio gradually declined and did not reach statistical significance.

To further investigate the specificity of FLT and FDG uptake for changes in tumor proliferation after chemoradiotherapy, we compared the radiotracer uptake for individual tumors with the corresponding changes in $LI_{Ki\text{-}67}$ within the same tumors (Fig. 3C-D). A strongly positive correlation was found between [^{3}H]FLT uptake in SEG-1 tumors and $LI_{Ki\text{-}67}$ (r = 0.89, P < 0.001). [^{3}H]FDG tumor uptake, however, weakly correlated with $LI_{Ki\text{-}67}$ (r = 0.39, P = 0.08).

Micro-PET studies. Figure 4 shows representative coronal and transverse micro-PET images of SEG-1 tumor-bearing mice

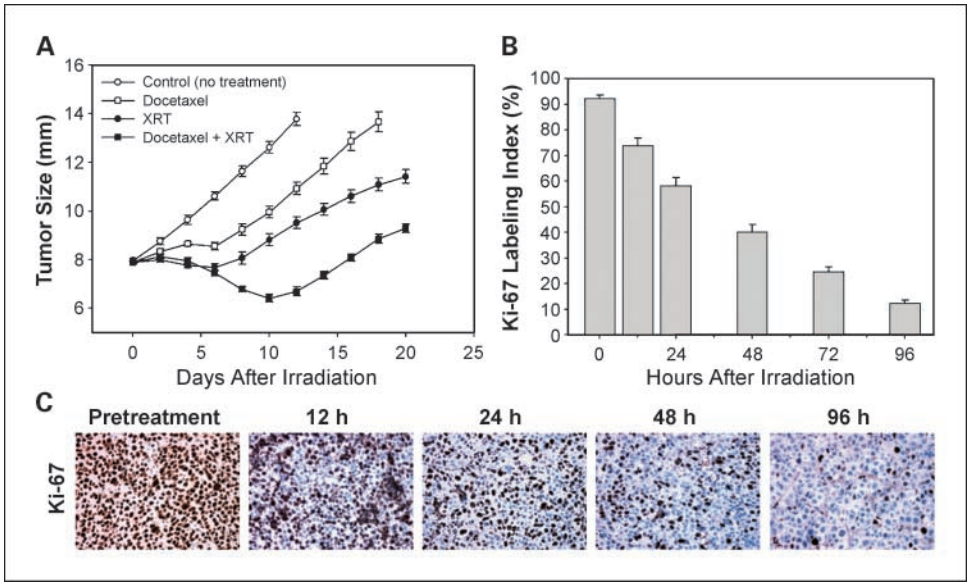

Fig. 2. Effect of docetaxel and radiation on growth and tumor proliferation in SEG-1 tumor xenografts. *A,* tumor growth delay after vehicle (no treatment), 33 mg/kg i.v. docetaxel, 15 Gy irradiation, or combination of docetaxel plus irradiation (n = 8 mice/group). *B,* changes in tumor proliferation (Ki-67) up to 96 hours after docetaxel plus irradiation (n = 5 mice/time point). Columns, mean; bars, SE. *C,* typical Ki-67-stained histologic sections of SEG-1 tumors 12 to 96 hours after docetaxel plus irradiation treatment are shown at ×40 magnification (×10 eyepiece). Differences in brown staining, differences in proliferation. Blue staining, hematoxylin counterstaining.

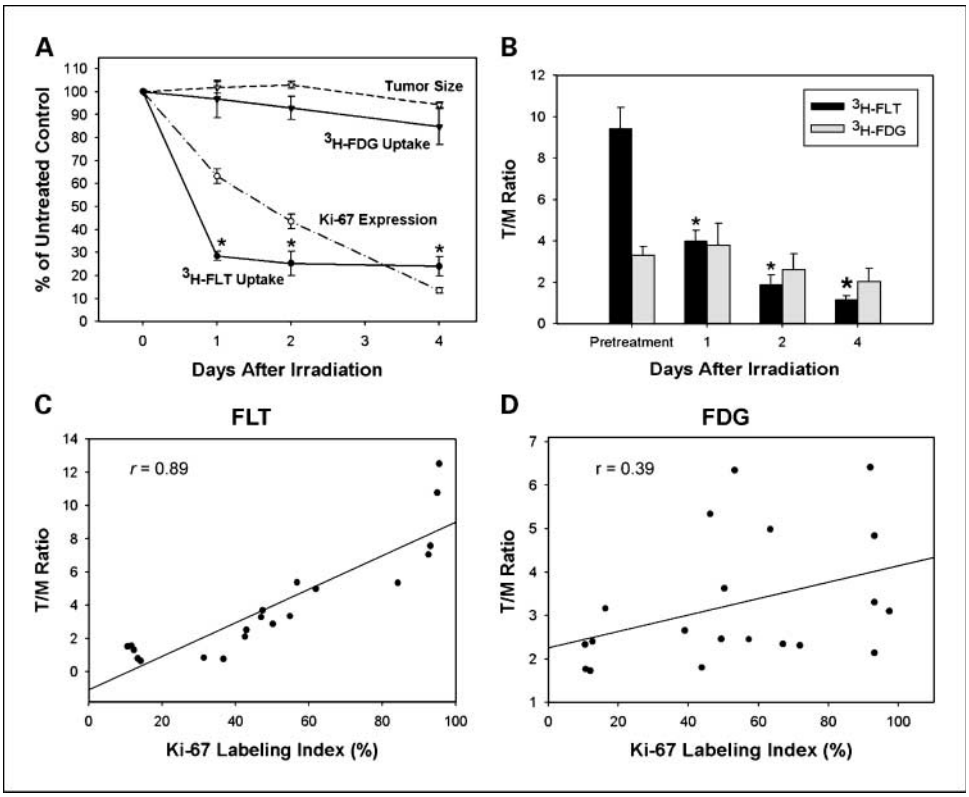

Fig. 3. Tumor uptake of [^{3}H]FLT and [^{3}H]FDG after docetaxel and radiation. *A*, effect of docetaxel plus irradiation on [^{3}H]FLT and [^{3}H]FDG uptake in excised SEG-1 xenografts (n = 5 mice/time point per radiotracer) shown up to 4 days after treatment. Tumor size and Ki-67 expression were also shown as independent measures of tumor response for correlation. Data are expressed as percentage uptake compared with untreated control tumors. *B*, tumor uptake of [^{3}H]FLT and [^{3}H]FDG normalized to muscle uptake and expressed as T/M uptake ratio. Columns, mean; bars, SE. *, $P < 0.005$, using ANOVA. Correlation between mean [^{3}H]FLT (*C*) and [^{3}H]FDG (*D*) T/M uptake ratios and Ki-67 labeling index within individual SEG-1 tumor xenografts.

at 1 hour after injection of [^{18}F]FLT and [^{18}F]FDG in untreated and 2 days postchemoradiotherapy animals. The micro-PET imaging data were in agreement with the *ex vivo* radiotracer uptake studies. Both [^{18}F]FLT (T/M uptake ratio 8.79) and [^{18}F]FDG (T/M uptake ratio 5.36) clearly visualized untreated control tumors implanted into the right hind limbs of the mice. Chemoradiotherapy markedly reduced tumor uptake of [^{18}F]FLT after 2 days, decreasing the T/M uptake ratio by −58%. The decrease in [^{18}F]FDG T/M uptake ratio was less pronounced (−17%) compared with [^{18}F]FLT reduction. The size of treated tumors did not significantly change in these mice, which was consistent with the tumor growth delay studies.

Imaging-histologic spatial correlation. Figure 5 shows preliminary data that the spatial distribution of [^{18}F]FLT uptake in untreated and chemoradiotherapy treated tumors correlated well with the spatial distribution of Ki-67 expression. The overall intensity of [^{18}F]FLT uptake in the autoradiographs of treated and 2 days postchemoradiotherapy tumors seemed consistent with the observed micro-PET images. Regions of high-intensity [^{18}F]FLT uptake in the autoradiographs exhibited prominent staining for Ki-67. This positive spatial correlation was also observed in intermediate- and low-intensity areas of [^{18}F]FLT uptake.

Discussion

This is the first study to provide preclinical evidence that FLT-PET accurately depicts early changes in tumor proliferation after chemoradiotherapy that precede tumor volume changes in *in vitro* and *in vivo* models of esophageal cancer. Our findings suggest that FLT-PET may be useful as a noninvasive imaging modality to assess early response to chemoradiotherapy in esophageal cancer. The ability of FLT-PET to detect response to chemoradiotherapy within days of treatment (after 48 hours) may allow physicians to overcome the inherent limitations imposed by conventional anatomic imaging and individualize therapeutic approaches according to whether tumors are chemoradioresponsive or chemoradioresistant. Specifically, the early identification of chemoradiotherapy responders and nonresponders would assist in avoiding unnecessary, highly morbid surgical procedures for responders (i.e., esophagectomy) and discontinuing ineffective neoadjuvant treatment regimens and instituting alternative therapies for nonresponders, thereby reducing delays in clinical management and potentially improving clinical outcomes in esophageal cancer.

The combination of docetaxel and radiation resulted in significant reduction of FLT uptake in tumors, which was depicted in our *in vitro* and *ex vivo* uptake and micro-PET imaging studies. When normalized to muscle tissue, FLT uptake in tumors in our *ex vivo* study decreased in a stepwise fashion with a sharp decline as early as 1 day after treatment, followed by a stable decline over the next 3 days. [^{18}F]FLT micro-PET showed the feasibility of imaging these changes. Importantly, these reductions in FLT tumor uptake were not secondary to decreases in tumor volume, because early reduction in FLT uptake occurred during the first few days of cytostatic tumor growth. Similar findings were reported in other FLT-PET preclinical studies that used different anticancer therapies, including chemotherapy (15, 16, 19) and radiation (12, 17). Our data lend further support to the literature showing the ability of FLT-PET to detect therapeutic alterations in tumor biology before changes in tumor size are clinically detectable. It is not clear at this point whether FLT uptake after

chemoradiotherapy differs from treatment with chemotherapy alone or radiation alone. The intent of the growth delay studies was to show the superior efficacy of combined docetaxel and radiation in our tumor model rather than to compare FLT uptake changes between the different treatment regimens. Future studies examining these differences would be interesting.

We validated the specificity of FLT-PET for depicting changes in tumor proliferation by demonstrating a significantly positive correlation between FLT tumor uptake reduction and conventional assessments of cellular proliferation. The dynamics of this reduction *in vitro* closely resembles the changes in [^{3}H]Thd tumor uptake after treatment, which is consistent with other *in vitro* comparative uptake studies of [^{3}H]FLT and [^{3}H]Thd (14, 20). Our data, however, are the first to establish that this correlation with Thd remains intact after anticancer treatment *in vitro*. The altered patterns of cell cycle distribution of SEG-1 cells after docetaxel (i.e., G_2-M cell cycle arrest) were also similar to findings in other published reports using taxanes (24, 25, 37). The reduction in G_1-S phase cells after docetaxel further supports the rationale for using FLT-PET to assess proliferative response after chemoradiotherapy, because cellular FLT uptake is dependent on late G_1-S phase specific expression of TK1 (21, 22).

It is interesting to note the initial increase in [^{3}H]FLT and [^{3}H]Thd uptake immediately after docetaxel that precedes their decline (Fig. 1). The cell cycle data also show a similar increase in S-phase cells, which suggests that this finding may be explained by an accumulation of S-phase cells as cells progress through the cell cycle beyond the G_2-M into S phase. This *in vitro* finding is in contrast to the early decreases in [^{3}H]FLT and Ki-67 observed in tumor xenografts after chemoradiotherapy. It must be pointed out, however, that the early decreases in proliferation *in vivo* are observed after the administration of both docetaxel and irradiation 24 hours later. Although we did not study the proliferative status of xenografts immediately after docetaxel alone, it is possible that a transient, initial increase in Ki-67 would also have been observed similar to *in vitro* studies.

A unique finding in our study was the spatial correlation between FLT uptake and Ki-67 expression distribution on autoradiography. Previous studies have shown the strong correlation between overall FLT tumor uptake and histologic assessment of cellular proliferation (Table 1). Although preliminary, our finding is the first evidence that this correlation also exists spatially for FLT-PET with reasonably high fidelity, adding to the robustness of FLT as an imaging surrogate of tumor proliferation. Furthermore, imaging-histologic correlation also buttresses the rationale and feasibility of delivering escalated doses of radiation to regions of high tumor proliferative activity in the clinical setting through conformal image-guided radiation therapy. A recent small pilot study that staged 10 esophageal cancer patients with the aid of [^{18}F]FLT and [^{18}F]FDG contradicts our results, reporting a negative correlation between [^{18}F]FLT and Ki-67 in biopsy specimens (38). The small number of patients and potential for sampling error in biopsy specimens in that study may have contributed to the discrepancy from our findings. Only a study involving more patients and tightly controlled tumor sampling protocols could resolve this discrepancy.

Although studies have shown that changes in [^{18}F]FDG uptake during neoadjuvant chemoradiotherapy are correlated with patient outcomes in esophageal cancer (2, 39, 40), other studies have suggested that [^{18}F]FDG may have difficulty in differentiating between complete responses and residual disease or posttreatment inflammation (6–8). Recent animal and preliminary clinical studies have suggested that [^{18}F]FLT may be an even more sensitive measure than [^{18}F]FDG for tumor response (12, 15–17, 19, 41–43). For example, Yang et al. (12) recently showed larger early decreases in [^{18}F]FLT uptake in SCCVII tumor-bearing mice after irradiation than in [^{18}F]FDG uptake. Leyton et al. (16) showed that [^{18}F]FLT was superior in assessing tumor proliferation compared with [^{18}F]FDG in RIF-1 tumor-bearing mice after cisplatin treatment (r = 0.89 versus r = 0.55, respectively). Similarly, we showed early decreases in FLT tumor uptake that were more pronounced and specific for tumor proliferation than those of FDG. Furthermore, when normalizing FLT uptake to background (muscle) uptake as was done in other studies (12, 18, 19), FLT displayed a much greater T/M signal contrast than FDG. Our data provide additional evidence for the assertion that imaging tumor proliferation with [^{18}F]FLT is more suitable for monitoring treatment response than imaging tumor glucose metabolism.

It should be noted that in our tumor models, the baseline absolute [^{3}H]FDG tumor uptake in our *in vitro* and *ex vivo* studies was low compared with absolute [^{3}H]FLT tumor uptake.

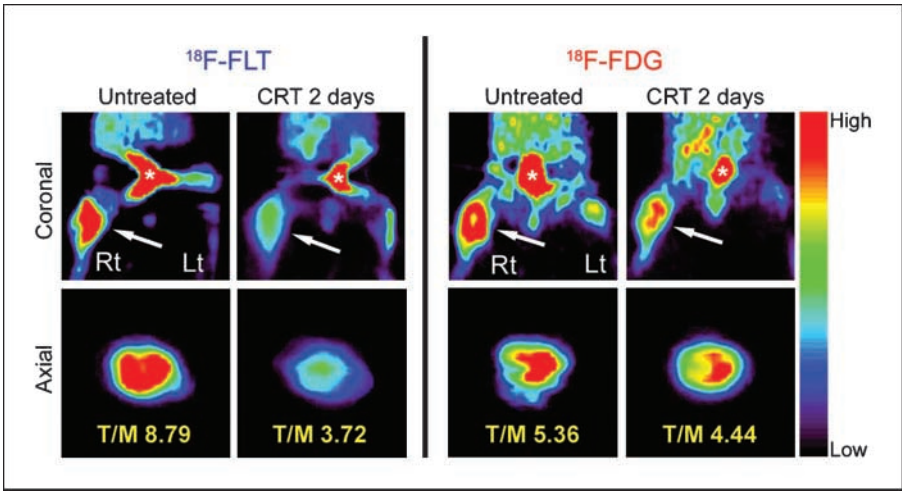

Fig. 4. [^{18}F]FLT and [^{18}F]FDG micro-PET imaging of SEG-1 tumor-bearing mice. Coronal (*top row*) and axial (*bottom row*) micro-PET sections of mice 1 hour after injection with [^{18}F]FLT (*left columns*) or [^{18}F]FDG (*right columns*) before treatment and 2 days after chemoradiation (*CRT*; n = 2 mice/group). Implanted tumors (*arrows*) are located on the right (*Rt*) hind limbs of mice. Color scale, high (*red*) and low (*purple*) radiotracer uptake. Tumor uptake of radiotracers is normalized to muscle radiotracer uptake and expressed as T/M uptake ratio. *, bladder.

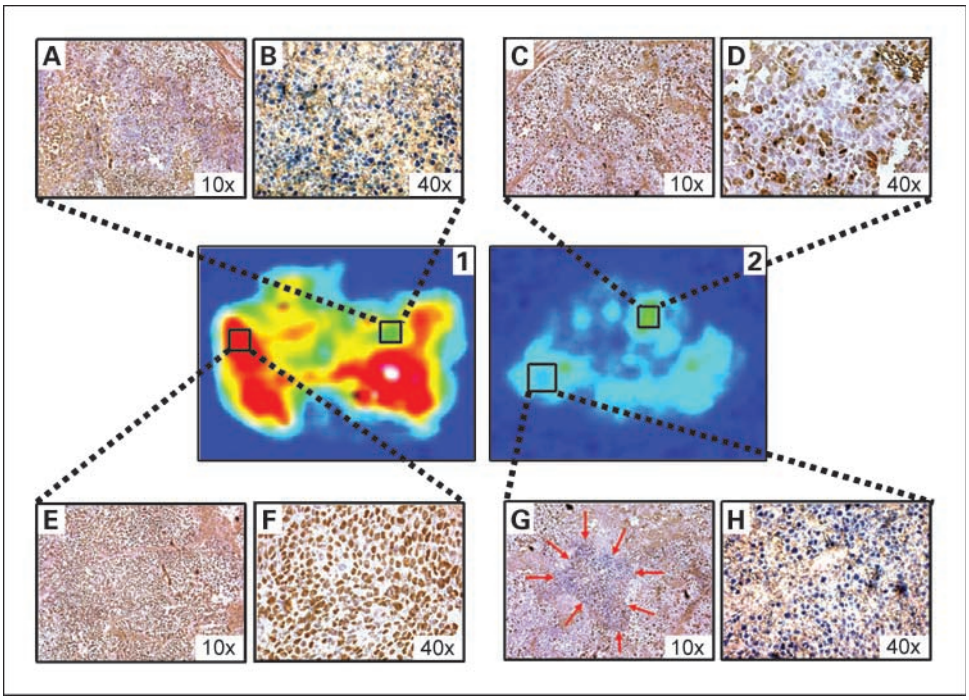

Fig. 5. Spatial correlation of [^{18}F]FLT uptake and Ki-67 expression distributions in autoradiographs of SEG-1 tumors. Middle, autoradiographs of untreated (*1*) and 2 days postchemoradiotherapy (*2*) tumors. Expression of Ki-67 by histologic examination is shown from selected areas of high (*E* and *F*), intermediate (*A* to *D*), and low (*G* and *H*) [^{18}F]FLT intensity uptake. Magnifications of Ki-67 staining are shown as insets in each panel. Cells stained brown, positive for Ki-67; cells stained blue, counterstained with hematoxylin. Arrows in (*G*) outline an island cluster of nonproliferating tumor cells. Color scale indicates high (*red*) and low (*purple*) [^{18}F]FLT uptake.

This is in contrast to several other studies comparing [^{18}F]FLT and [^{18}F]FDG tumor uptake in which the absolute [^{18}F]FDG tumor uptake was ~1.5 to 5× greater than that of [^{18}F]FLT (15–17, 42). It is possible that some of the ^{3}H labeled to FDG in our experiments may have exchanged with water and resulted in decreased ^{3}H counts within the cells or tumors at baseline. However, any potential errors arising from this phenomenon would likely have been eliminated by the use of the T/M uptake ratio, as this [^{3}H]water exchange would also have occurred in muscle tissue and thus canceled each other. It is also possible that, similar to the low baseline [^{18}F]FDG uptake observed in the Waldherr et al. study (19), SEG-1 tumor cells in our study had low FDG uptake as well. However, this is unlikely considering the relatively high tumor uptake of [^{18}F]FDG in our micro-PET imaging study.

In conclusion, this present study showed that FLT-PET is suitable for depicting early reductions in tumor proliferation (48 hours after chemoradiotherapy) in preclinical models of esophageal cancer after chemoradiotherapy before changes in tumor size are evident. We conclude that FLT-PET is superior to FDG-PET as a noninvasive imaging tool to assess early tumor proliferative responses to chemoradiotherapy. Additional studies are ongoing to further determine whether FLT-PET can distinguish between varying degrees of treatment response and predict for pathologic complete response as well as detect early biological changes during the regrowth phase after ineffective

Table 1. Correlation between FLT tumor uptake and histologic proliferative markers in published literature

Study	Disease site	Proliferation correlation		FDG correlation
		Marker	Correlation	
Barthel et al. (15)*	Fibrosarcoma	PCNA	$r = 0.71$	$r = 0.53$
Waldherr et al. (19)*	SCCa	PCNA	$r = 0.71$	$r = 0.74$
Leyton et al. (16)*	Fibrosarcoma	PCNA	$r = 0.89$	$r = 0.55$
Wagner et al. (44)*†	Lymphoma	BrdUrd*	$r = 0.63$	
		Ki-67†	$r = 0.95$	
Vesselle et al. (45)†	Lung	Ki-67	$r = 0.84$	
Buck et al. (42)†	Lung	Ki-67	$r = 0.92$	$r = 0.59$
Francis et al. (43)†	Colon	Ki-67	$r = 0.80$	$r = 0.40$
Cobben et al. (46)†	Sarcoma	Ki-67	$r = 0.65$	
van Westreenen et al. (38)†	Esophageal	Ki-67	$r = -0.76$	$r = 0.14$

Abbreviations: BrdUrd, bromodeoxyuridine; PCNA, proliferating cell nuclear antigen; SCCa, squamous cell carcinoma.
*Preclinical.
†Clinical.

therapy. Imaging-pathologic studies in patients with esophageal cancer are also under way to validate the sensitivity and specificity of FLT-PET in patients receiving chemoradiotherapy. If these endeavors are successful, they may allow physicians to tailor chemoradiotherapy regimens during the early phase of a treatment course and avoid ineffective and morbid therapies.

Acknowledgments

We thank Nancy Hunter, Bobby Neal, and David Valdecanas for their invaluable assistance in the animal studies; Kuriakose Abraham for his expertise in processing histologic specimens; Dr. Nicholas Terry and Nalini Patel for their help in the immunohistochemistry and flow cytometry studies; and Walter J. Pagel for his assistance in manuscript editing.

References

1. Urba SG, Orringer MB, Turrisi A, et al. Randomized trial of preoperative chemoradiation versus surgery alone in patients with locoregional esophageal carcinoma. J Clin Oncol 2001;19:305–13.
2. Swisher SG, Erasmus J, Maish M, et al. 2-Fluoro-2-deoxy-D-glucose positron emission tomography imaging is predictive of pathologic response and survival after preoperative chemoradiation in patients with esophageal carcinoma. Cancer 2004;101:1776–85.
3. Ancona E, Ruol A, Santi S, et al. Only pathologic complete response to neoadjuvant chemotherapy improves significantly the long term survival of patients with resectable esophageal squamous cell carcinoma: final report of a randomized, controlled trial of preoperative chemotherapy versus surgery alone. Cancer 2001;91:2165–74.
4. Berger AC, Farma J, Scott WJ, et al. Complete response to neoadjuvant chemoradiotherapy in esophageal carcinoma is associated with significantly improved survival. J Clin Oncol 2005;23:4330–7.
5. Westerterp M, van Westreenen HL, Reitsma JB, et al. Esophageal cancer: CT, endoscopic US, and FDG PET for assessment of response to neoadjuvant therapy-systematic review. Radiology 2005;236:841–51.
6. Arslan N, Miller TR, Dehdashti F, Battafarano RJ, Siegel BA. Evaluation of response to neoadjuvant therapy by quantitative 2-deoxy-2-[18f]fluoro-D-glucose with positron emission tomography in patients with esophageal cancer. Mol Imaging Biol 2002;4:301–10.
7. Kubota R, Yamada S, Kubota K, et al. Intratumoral distribution of fluorine-18-fluorodeoxyglucose *in vivo*: high accumulation in macrophages and granulation tissues studied by microautoradiography. J Nucl Med 1992;33:1972–80.
8. Nakamura R, Obara T, Katsuragawa S, et al. Failure in presumption of residual disease by quantification of FDG uptake in esophageal squamous cell carcinoma immediately after radiotherapy. Radiat Med 2002;20:181–6.
9. Begg AC. Prediction of repopulation rates and radiosensitivity in human tumours. Int J Radiat Biol 1994;65:103–8.
10. Krohn KA, Mankoff DA, Eary JF. Imaging cellular proliferation as a measure of response to therapy. J Clin Pharmacol 2001;41:96S–103S.
11. Dittmann H, Dohmen BM, Kehlbach R, et al. Early changes in [18F]FLT uptake after chemotherapy: an experimental study. Eur J Nucl Med Mol Imaging 2002;29:1462–9.
12. Yang YJ, Ryu JS, Kim SY, et al. Use of 3′-deoxy-3′-[(18)F]fluorothymidine pet to monitor early responses to radiation therapy in murine SCCVII tumors. Eur J Nucl Med Mol Imaging 2006;33:412–9.
13. Shields AF, Grierson JR, Dohmen BM, et al. Imaging proliferation *in vivo* with [F-18]FLT and positron emission tomography. Nat Med 1998;4:1334–6.
14. Toyohara J, Waki A, Takamatsu S, et al. Basis of FLT as a cell proliferation marker: comparative uptake studies with [^{3}H]thymidine and [^{3}H]arabinothymidine, and cell-analysis in 22 asynchronously growing tumor cell lines. Nucl Med Biol 2002;29:281–7.
15. Barthel H, Cleij MC, Collingridge DR, et al. 3′-Deoxy-3′-[18F]fluorothymidine as a new marker for monitoring tumor response to antiproliferative therapy *in vivo* with positron emission tomography. Cancer Res 2003;63:3791–8.
16. Leyton J, Latigo JR, Perumal M, et al. Early detection of tumor response to chemotherapy by 3′-deoxy-3′-[18f]fluorothymidine positron emission tomography: the effect of cisplatin on a fibrosarcoma tumor model *in vivo*. Cancer Res 2005;65:4202–10.
17. Sugiyama M, Sakahara H, Sato K, et al. Evaluation of 3′-deoxy-3′-18F-fluorothymidine for monitoring tumor response to radiotherapy and photodynamic therapy in mice. J Nucl Med 2004;45:1754–8.
18. Oyama N, Ponde DE, Dence C, et al. Monitoring of therapy in androgen-dependent prostate tumor model by measuring tumor proliferation. J Nucl Med 2004;45:519–25.
19. Waldherr C, Mellinghoff IK, Tran C, et al. Monitoring antiproliferative responses to kinase inhibitor therapy in mice with 3′-deoxy-3′-18F-fluorothymidine pet. J Nucl Med 2005;46:114–20.
20. Rasey JS, Grierson JR, Wiens LW, Kolb PD, Schwartz JL. Validation of FLT uptake as a measure of thymidine kinase-1 activity in a549 carcinoma cells. J Nucl Med 2002;43:1210–7.
21. Sherley JL, Kelly TJ. Regulation of human thymidine kinase during the cell cycle. J Biol Chem 1988;263:8350–8.
22. Munch-Petersen B, Cloos L, Jensen HK, Tyrsted G. Human thymidine kinase 1. Regulation in normal and malignant cells. Adv Enzyme Regul 1995;35:69–89.
23. Milas L, Milas MM, Mason KA. Combination of taxanes with radiation: preclinical studies. Semin Radiat Oncol 1999;9:12–26.
24. Dunne AL, Mothersill C, Robson T, Wilson GD, Hirst DG. Radiosensitization of colon cancer cell lines by docetaxel: mechanisms of action. Oncol Res 2004;14:447–54.
25. Suzuki M, Nakamatsu K, Kanamori S, Masunaga S, Nishimura Y. Additive effects of radiation and docetaxel on murine sccvii tumors *in vivo*: special reference to changes in the cell cycle. Radiat Res 2003;159:799–804.
26. Mason KA, Hunter NR, Milas M, Abbruzzese JL, Milas L. Docetaxel enhances tumor radioresponse *in vivo*. Clin Cancer Res 1997;3:2431–8.
27. Mason KA, Kishi K, Hunter N, et al. Effect of docetaxel on the therapeutic ratio of fractionated radiotherapy *in vivo*. Clin Cancer Res 1999;5:4191–8.
28. Mason K, Staab A, Hunter N, et al. Enhancement of tumor radioresponse by docetaxel: involvement of immune system. Int J Oncol 2001;18:599–606.
29. Rigas JR, Dragnev KH, Bubis JA. Docetaxel in the treatment of esophageal cancer. Semin Oncol 2005;32:S39–51.
30. Pasini F, de Manzoni G, Pedrazzani C, et al. High pathological response rate in locally advanced esophageal cancer after neoadjuvant combined modality therapy: dose finding of a weekly chemotherapy schedule with protracted venous infusion of 5-fluorouracil and dose escalation of cisplatin, docetaxel and concurrent radiotherapy. Ann Oncol 2005;16:1133–9.
31. Ajani JA, Fodor MB, Tjulandin SA, et al. Phase ii multi-institutional randomized trial of docetaxel plus cisplatin with or without fluorouracil in patients with untreated, advanced gastric, or gastroesophageal adenocarcinoma. J Clin Oncol 2005;23:5660–7.
32. Martin SJ, Eisenbarth JA, Wagner-Utermann U, et al. A new precursor for the radiosynthesis of [18F]FLT. Nucl Med Biol 2002;29:263–73.
33. Hughes SJ, Nambu Y, Soldes OS, et al. Fas/apo-1 (cd95) is not translocated to the cell membrane in esophageal adenocarcinoma. Cancer Res 1997;57:5571–8.
34. Sasajima T, Miyagawa T, Oku T, et al. Proliferation-dependent changes in amino acid transport and glucose metabolism in glioma cell lines. Eur J Nucl Med Mol Imaging 2004;31:1244–56.
35. Key G, Meggetto F, Becker MH, et al. Immunobiochemical characterization of the antigen detected by monoclonal antibody ind.64. Evidence that ind.64 reacts with the cell proliferation associated nuclear antigen previously defined by ki-67. Virchows Arch B Cell Pathol Incl Mol Pathol 1992;62:259–62.
36. Meyn RE, Stephens LC, Hunter NR, Ang KK, Milas L. Reemergence of apoptotic cells between fractionated doses in irradiated murine tumors. Int J Radiat Oncol Biol Phys 1994;30:619–24.
37. Milross CG, Mason KA, Hunter NR, et al. Enhanced radioresponse of paclitaxel-sensitive and -resistant tumours *in vivo*. Eur J Cancer 1997;33:1299–308.
38. van Westreenen HL, Cobben DC, Jager PL, et al. Comparison of ^{18}F-FLT PET and ^{18}F-FDG pet in esophageal cancer. J Nucl Med 2005;46:400–4.
39. Weber WA, Ott K, Becker K, et al. Prediction of response to preoperative chemotherapy in adenocarcinomas of the esophagogastric junction by metabolic imaging. J Clin Oncol 2001;19:3058–65.
40. Wieder HA, Brucher BL, Zimmermann F, et al. Time course of tumor metabolic activity during chemoradiotherapy of esophageal squamous cell carcinoma and response to treatment. J Clin Oncol 2004;22:900–8.
41. van Waarde A, Cobben DC, Suurmeijer AJ, et al. Selectivity of ^{18}F-FLT and ^{18}F-FDG for differentiating tumor from inflammation in a rodent model. J Nucl Med 2004;45:695–700.
42. Buck AK, Halter G, Schirrmeister H, et al. Imaging proliferation in lung tumors with PET: ^{18}F-FLT versus ^{18}F-FDG. J Nucl Med 2003;44:1426–31.
43. Francis DL, Freeman A, Visvikis D, et al. *In vivo* imaging of cellular proliferation in colorectal cancer using positron emission tomography. Gut 2003;52:1602–6.
44. Wagner M, Seitz U, Buck A, et al. 3′-[18F]fluoro-3′-deoxythymidine ([18F]-FLT) as positron emission tomography tracer for imaging proliferation in a murine B-cell lymphoma model and in the human disease. Cancer Res 2003;63:2681–7.
45. Vesselle H, Grierson J, Muzi M, et al. *In vivo* validation of 3′deoxy-3′-[(18)F]fluorothymidine ([(18)F]FLT) as a proliferation imaging tracer in humans: correlation of [(18)F]FLT uptake by positron emission tomography with Ki-67 immunohistochemistry and flow cytometry in human lung tumors. Clin Cancer Res 2002;8:3315–23.
46. Cobben DC, Elsinga PH, Suurmeijer AJ, et al. Detection and grading of soft tissue sarcomas of the extremities with (18)F-3′-fluoro-3′-deoxy-L-thymidine. Clin Cancer Res 2004;10:1685–90.